Nordic Journal of Surveying and Real Estate Research 6:1 (2009) 21–39
submitted on May 23, 2008
revised on September 29, 2008
accepted on October 3, 2008

Consequence of DTM Precision for Flood Hazard Mapping: A Case Study in SW Finland

Petteri Alho[1], Hannu Hyyppä[2] and Juha Hyyppä[3]
[1]University of Turku, Department of Geography, FI-20014 University of Turku, petteri.alho@utu.fi
[2]Helsinki University of Technology, Research Institute for Modelling and Measuring for the Built Environment, P.O. Box 1200, FI-02015 HUT, hannu.hyyppa@tkk.fi
[3]Finnish Geodetic Institute, Department of Remote Sensing and Photogrammetry, Geodeetinrinne 2, P.O. Box 15, FI-02431 Masala, juha.hyyppa@fgi.fi

Abstract. *Spatial information on floods, which includes inundation maps and estimations of flood damage are essential tools for the creation of effective plans for both flood protection and mitigation. In flood modelling, the accuracy of the model geometry used has a remarkable impact upon flood mapping. Therefore, in this study, flood hazard mapping was undertaken with two existing DTM (digital terrain model) products and a high-precision LiDAR-based DTM. Their characteristics were evaluated with respect to flood hazard mapping. An accuracy assessment of these digital terrain models and their applicability for one-dimensional flood inundation mapping clearly showed that LiDAR DTM topography was the most applicable. Although the 10×10 m DTM from the Finnish National Land Survey could be utilised to show where flooding might occur for very coarse flood mapping surveys, these were not suitable for more exact estimations of flood boundaries. Nevertheless, some inaccuracies in riverbank topography were also found using the LiDAR-DTM. Hence, to study detailed hydrological processes such as short-term channel dynamics, this particular DTM could be further improved by additional data.*

Keywords: *Flood mapping, DTM, LiDAR, Finland.*

1 Introduction & background

Floods are the main natural hazard in Europe, more than one hundred events having occurred between 1998 and 2002, which caused major damage and loss of life (*ca*. 700 casualties), the displacement of half a million people and financial losses in excess of €25 billion (EC 2005). In 2005, flood damages reached at least 1.1 billion euros in Europe (Dartmouth Flood Observatory 2008). It has been estimated that extreme flood events (HQ 1/250a) could cause damages of up to €550 million in

Finland (Ollila et al., 2000). Recently, losses incurred include *ca*. 7 million euros in southern Finland in the summer of 2004 and *ca*. 5 million euros in Finnish Lapland in the spring of 2005. These damages have had a serious impact at a local scale. Due to such flood hazards, the European Union has strengthened work for flood protection and mitigation, resulting in the European Union flood directive (Directive on 2007/60/EC, 2007). This directive obliges member states to carry out flood hazard mapping (see definition below) and create flood mitigation plans for all significant flooding areas. Finnish authorities have decided to undertake these flood mapping procedures with existing data and 1D-hydraulic modelling or simple water surface interpolation (cf. Sane et al., 2006). Furthermore, in Finland preliminary results indicate that climate change increases flood discharges and hence, flood damages (Veijalainen & Vehviläinen, 2007; Alho et al., 2007). Therefore, spatial information on floods, including flood inundation maps and estimations of flood-induced damages are essential tools for creating effective flood protection plans as well as flood mitigation measures.

While the terms 'flood mapping', 'flood risk', and 'flood hazard' have been broadly used in digitally-aided flood mapping, these expressions have been only recently defined internationally by both the EC (2005) and Floodsite (2005) and nationally by the EXTREFLOOD research project (Sane et al., 2006). There are two different main products of flood mapping: (1) the flood hazard map, which is defined as a map showing those areas where floods have to be considered, with or without (according Floodsite, 2005) indication of flood probability and the degree of danger (e.g. water depth, flow velocity or a combination of both) (Sane et al., 2006). (2) The flood risk map, defined as a map showing the inundated area and flood damages (Alho et al., 2008). The flood risk map represents flood damages with a certain return period (cf. HQ 1/100a). In other words, the flood risk map is a function of both flood hazard and vulnerability (populace, infrastructure, financial damages or environmental hazards) (cf. Floodsite, 2005; Alho et al., 2008).

Formerly, topographic data have been acquired by time-consuming ground surveys or alternatively from national topographic maps. To date, the most common digital elevation models available in Finland are those produced by the National Land Survey of Finland (NLS). These digital elevation data are not suitable for detailed hydraulic modelling or flood mapping, because they represent generalised topography and do not include details of riverbanks or embankments, and because even a general elevation for a low-lying, level area may be strongly erroneous (Sane et al. 2006). Therefore, in the case of flood modelling, the high-accurate processed LiDAR-DTM data on Finland should be evaluated.

Airborne laser scanning (ALS) data has been used successfully in the assessment of topographic data for over a decade, while ground survey methods can be applied for smaller areas using either terrestrial (TLS) or vehicle-based laser scanning. Recently, several countries have performed nationwide ALS surveys, primarily for DTM purposes. These countries include the Netherlands, Switzerland, Germany and several states in the USA. In the Netherlands, the national laser scanning was initiated to meet the demand for detailed and up-to-date elevation information from the water boards, provinces and the Ministry of Transport (Rijkswaterstaat). The Dutch DTM was collected with a relatively sparse point cloud. Today, the preferred point cloud density is about 0.5–1 point per m^2. The National Land Survey of Finland has also initiated the collection of nationwide elevation data: 20,000 km^2 of data will be collected in 2008. Obtaining highly accurate DTM's in flood risk areas is the driving force of the data acquisition and the quality of the new ALS-based elevation model in Finland will surpass 30 cm. Preliminary studies by Ahokas et al. (2008) in the Salo test area have shown that possible levels of accuracy may even reach from 10 to 15 cm in elevation for vegetated areas during the leafless season.

DTM characteristics have a major impact on environmental modelling (Fisher & Tate 2006). A number of studies have also been done to demonstrate the effect of the DTM characteristics in hydrological studies (e.g. Alsdorf et al., 2000; Kenward et al., 2000; Cobby et al., 2001; Bates et al., 2003, Hudson & Colditz, 2003; Ludwig & Schneider, 2006; Sanders, 2007). Bates (2004) stated that hydraulic models which can be used for flood inundation mapping require four input data types: (1) topographic data to create the model geometry; (2) bulk flow data to provide both model inflow and outflow boundary conditions; (3) an estimate of the grid-square effective friction parameter for each model cell; (4) a source of validation data. Schumann et al. (2008) have tested the approach to estimate flood stage based on flood boundary information and different types of elevation data. They pointed out that to derive useful information on hydraulic modelling, such as water stages, uncertainties and scaling issues of the DTM need to be well understood and sufficiently accounted for. Sanders (2007) demonstrated on-line sources of the DTM's in the United States and tested flood inundation estimation with 2D hydraulic modelling (steady and unsteady scheme) and field-based high water marks. He remarks that lower-precision digital elevation data normally enlarge inundated area in flood mapping and the best results could be acquired with LiDAR-DTM. Horritt and Bates (2002) have evaluated predictive flood inundation mapping with 1D and 2D models (HEC-RAS, LISFLOOD-FP and TELEMAC-2D) on a 60 km reach of the river Severn, UK. Their results show that both the HEC-RAS (1D model) and TELEMAC-2D (2D finite element model) models can be calibrated against discharge or inundated area data and give appropriate predictions of inundated area, whereas LISFLOOD-FP (2D raster based model) needs to be calibrated against independent inundated area data to produce acceptable results.

In this study, we evaluated differences in flood inundation mapping caused by the precision and the resolution of various digital terrain models in the Salo test area, SW Finland. We utilised existing 25×25 m and 10×10 m DTM's produced by the National Land Survey of Finland (NLS) and a more detailed DTM based on a pilot laser scanning by the NLS to produce 1/100a flood hazard maps combined with a simple 1-D hydraulic modelling approach. The 1-D modelling approach was used here as it will be utilised for flood mapping following the EU directive in Finland, and hence accuracy assessment of the different hydraulic modelling approaches (1-, 2-, 3-dimensional) is beyond the aim of this paper. Finally, we aimed to provide a scale-dependent recommendation for DTM usage in one dimensional flood hazard mapping and discuss how this fits in future planning of both the flood mapping and laser scanning campaigns in Finland.

2 Salo test area

Few floods have occurred recently in the city of Salo (southern Finland), situated in the drainage basin (570 km^2) of the Uskelanjoki River and lying on Viurilanlahti Bay (Fig. 1). The most extensive flood events which covered the Meriniitty area occurred in 1973. Nowadays, this area is occupied by industrial building complexes. Recent flooding events have as yet been minor, involving ice jamming problems in the city centre in late winter 1989 and partial flooding of the lower Meriniitty area in January 2005 (HQ 1/35a).

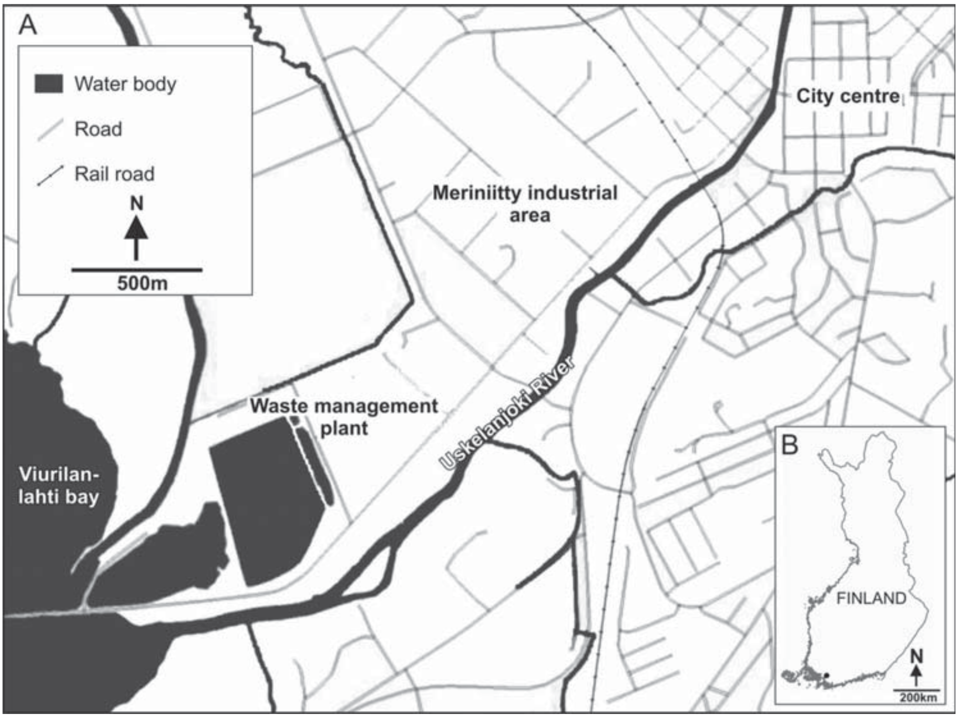

Figure 1. *The Salo study area is situated in SW Finland (Fig. 1B). The Uskelanjoki River flows through Salo and the city centre is located in the north eastern part of the map (Fig1A). The Helsinki–Turku railway line runs north-south through the city.*

However, a certain flooding risk does exist in this urban area. High sea water levels in Viurilanlahti Bay coupled with a high discharge from the Uskelanjoki River may cause flooding in the vicinity of the city centre. Furthermore, ice jamming may constitute a flood risk in the city centre as has already been recorded in 1989. The projected flood discharges are also significantly higher than present-day 1/100a and 1/250a flood discharges (Veijalainen, 2005). These discharge estimates are based on the Watershed Simulation and Forecast System (WSFS) developed by Finnish Environment Institute. WSFS is a HBV type conceptual hydrological model, which is used for operational flood forecasting in Finland. The

WSFS model uses observed values and forecasts from the Finnish Meteorological Institute to make forecasts for all important rivers and lakes of Finland. It has been calibrated with 20 years of weather, snow water equivalent, discharge and water level measurement data and performs well in present conditions in the test basins (Veijalainen, 2005). The system can offer hydrological estimates of extreme floods. However, the projected discharge may have remarkable variation depending on the used climate change scenario.

One of the primary reasons to select the Salo area in this research is because it was used in a pilot laser scanning campaign carried out by the Finnish National Land Survey (NLS) and Finnish Geodetic Institute in 2006–2007. In addition, 10×10 m and 25×25 m DTM products are available in the Salo area. The 1,200 km^2 test site near Salo had already been partly scanned in December 2006 using an Optech ALTM 3100 airborne laser scanner, with the remaining area surveyed later in May 2007 using the Leica ALS-50 system. Overlapping areas were partially covered using both scanning systems. A flight altitude of 2,000 m was used in the May 2007 test and flight parameters were similar to those used in the national laser scanning campaign. Laser scanning was carried out at altitudes of 500, 2,000 and 5,000 m. This test site served to analyse different laser acquisition parameters and to optimise flood modelling. However, analyses of the different laser acquisition parameters lay beyond the remit of this study and hence, only laser scanning data acquired from 5,000 m was used. Both this elevation and the acquisition parameters were broadly similar to the national laser scanning campaign undertaken by the NLS.

3 Material & Methods

3.1 25×25 m and 10×10 m DTM's

A 25×25 m digital terrain model product of the NLS covers the whole of Finland and has been produced from digitised contour lines of the topographic map and water body elements at scales of 1:10,000 and 1:20,000, respectively (NLS, 2007). The mean accuracy and standard deviation of the DTM product countrywide is 1.76 ± 1.39 m. The 25×25 m DTM has been divided into three accuracy groups (NLS, 2007): (1) more accurate than the mean value 1.76 m; (2) less accurate than 1.76 m but better than 10 m, and (3) Worse than 10 m accuracy. The Salo test area belongs to the first group. In the present study, a pre-analysis of the 25 m DTM accuracy showed that because 2.5 metre contour lines had not been utilised in the DTM production, the Uskelanjoki river valley was 2–2.5 metres too high along the downstream portion of the river. Furthermore, riverbanks were not modelled in the DTM.

The production of a national 10×10 m DTM began in the 2001 National Land Survey, with production based on digital Espa stereo stations. This method used stereo images for correcting contour lines obtained from old base maps. The applied scale for aerial images was 1:16,000. The contour lines were also improved using measured known points in the terrain, heights of water body boundaries and other known height information. The accuracy of the 10×10 m DTM is 1.1 m (Oksanen and Sarjakoski, 2006).

3.2 Lidar DTM

Airborne laser scanning (ALS) data has been used successfully in the assessment of topographic data for over a decade, while ground survey methods can be applied for smaller areas using either terrestrial (TLS) or vehicle-based laser scanning. ALS has been demonstrated as functional in producing high quality 3-D models of forested environments. Reutebuch et al. (2003) reported random errors of 14 cm for clear-cut, 14 cm for heavily thinned forest, 18 cm for lightly thinned forest and 29 cm for uncut forest using TopEye laser data with four pulses per square metre. However, in dense forests, errors up to 10 to 20 m can occur in the DTM data (Takeda, 2004). Hyyppä et al. (2005) concluded that in the boreal forest zone, random errors of less than 20 cm are obtained under most conditions for level terrain with a pulse density higher than 2 points/m^2. The increase in flight altitude from 400 (8 to 10 points/m^2) to 1,500 m (2 to 3 points/m^2) increased the random error in the derivation of digital terrain models from 12 to 18 cm (i.e. 50%). Thus, to improve DTM errors by a factor of two requires a significant increase in the PRF (pulse repetition frequency). There are systematic shifts in the elevation models derived at various flight altitudes and these systematic errors increase when the flight altitude increases. A detailed comparison of the filtering techniques used for DTM extraction was made within an ISPRS (International Society for Photogrammetry and Remote Sensing) filter evaluation (Sithole and Vosselman 2004). Examples of commercial software that includes DTM generation include REALM, TerraScan, Geomatica LidarEngine and SCOP++.

The processing of LiDAR digital terrain models included geoid correction, strip adjustment using overlapping strips and TerraMatch software and systematic shift corrections using ground control points. This was followed by the classification of laser point clouds using TerraScan software to separate the ground points from others, i.e. water body, low and high vegetation. The ground points were triangulated using the TIN (triangulated irregular network) densification algorithms of the TerraScan programme developed originally by Axelsson (2000). The DTM surface was allowed to fluctuate within certain values, controlled by minimum description length, constrained spline functions and active contour models for elevation differences. Selected ground points were connected in a TIN. An initial TIN was derived from neighbourhood minima, and then progressively densified into the laser point cloud. At each iteration, more points were added to the TIN, if they fell within defined thresholds. When compared with other algorithms used by Ahokas et al. (2002) for forested hills in Finland, this approach was found to be high in quality.

3.3 Pre-processing and accuracy assessment of the DTM's

The standard product of the DTM grids was not suitable for hydraulic modelling. Therefore, some pre-processing of the DTM was undertaken. The DTM's were converted to TIN format and improved by adding bathymetric data which extended from the mouth of the Uskelanjoki River to Viurilanlahti Bay and included 3 km of detailed channel bed geometry as breaklines and bulk points (*ca*. 2 points/m^2). Thus, both the river bed and portions of the riverbanks have exactly the same topography based on field-surveyed breaklines in all three DTM's, which, in turn, were utilised to define three different geometries for hydraulic modelling.

Prior to hydraulic modelling, an assessment of DTM accuracy was carried out against RTK-GPS (real-time kinematic GPS) measurements, which themselves were accurate to ±2 cm. In total, 196 RTK-points were surveyed in the Salo region. These points were partially surveyed at random with the remainder gathered from those features which had an integral role in flood inundation, i.e. banks, embankments, etc.

3.4 HEC-RAS modelling and flood inundation mapping

Hydraulic modelling was undertaken with the HEC-RAS 4.0 software, which is a one-dimensional hydraulic model for steady and unsteady flow situations in a channel network. The computation of unsteady flow is based on the conservation of mass and momentum and solved with Saint-Venant equations using the implicit finite difference method. Structures such as storage areas, pump stations, bridges, culverts, weirs and embankments may be included in the model. Steady flow computation, used in this study, is based on the standard step method (for a further description, see Hydrological Engineering Centre, 2002). The following standard assumptions are made when using the HEC-RAS hydraulic calculations in natural channels: (1) constant flow occurs along the whole reach, (2) flow varies gradually between cross-sections, (3) flow is one-dimensional, (4) slope gradients are less than 10%, and (5) the energy slope between cross-sections is constant (Hydrological Engineering Centre, 2002).

Input data of the hydraulic model, such as channel geometry derived from TIN, as well as surface roughness (Manning's *n*-value, friction parameter for hydraulic calculations, cf. Chow, 1959), were defined with HEC-GeoRAS (cf. Hydrologic Engineering Centre, 2002), which is an extension of Arc-GIS software. A total of 23 cross-sections were digitised in 3-D, with 34 cross-sections automatically interpolated along a reach of 4.2 km of the Uskelanjoki River. There was a mean distance of 74 m between the cross-sections. Surface roughness data was estimated from both a generalised SLICES database and aerial photo interpretation. This database was divided into 5 roughness classes based on land-use type. The flood model was calibrated against a 1/35a flood (91 $m^3 s^{-1}$ discharge) that occurred in the Salo region on the 9th of January, 2005. The extension of the flood and flood elevation was surveyed along the downstream part of the reach. These field-surveyed high water marks were used for adjusting of Manning's *n*-values to the acquired correct water surface elevation in 1/35a flood. This rather unusual flood event gave good calibration for a larger flood modelling set-up (HQ 1/100a, in this study). This calibrated 1D model was calculated with all three modelling geometries (all three DTM's). Subsequently, the modelled water surface elevations were interpolated to water surface grids in HEC-GeoRAS and differences of these flood inundation grids were compared in this study.

4 Results

4.1 Accuracy assessment of the DTM's

The LiDAR DTM clearly showed the best accuracy statistics (Table 1a), with maximum and minimum errors of 0.73 and –0.60 m, respectively, and a standard deviation of 0.19 m. Overall the results of the present work are comparable with those of Ahokas et al. (2008).

The other two digital terrain models showed worse accuracy statistics, i.e., between a four- and tenfold accuracy decrease. Another accuracy assessment analysis undertaken without 17 elevation points of the riverbanks indicated much better accuracy for the LiDAR DTM. Here, the maximum and minimum errors diminished to 0.39 and –0.35 m, respectively, with a standard deviation of 0.12 m. Furthermore, both the 25 m and 10 m DTM's showed better accuracy without these riverbank points (Table 1b).

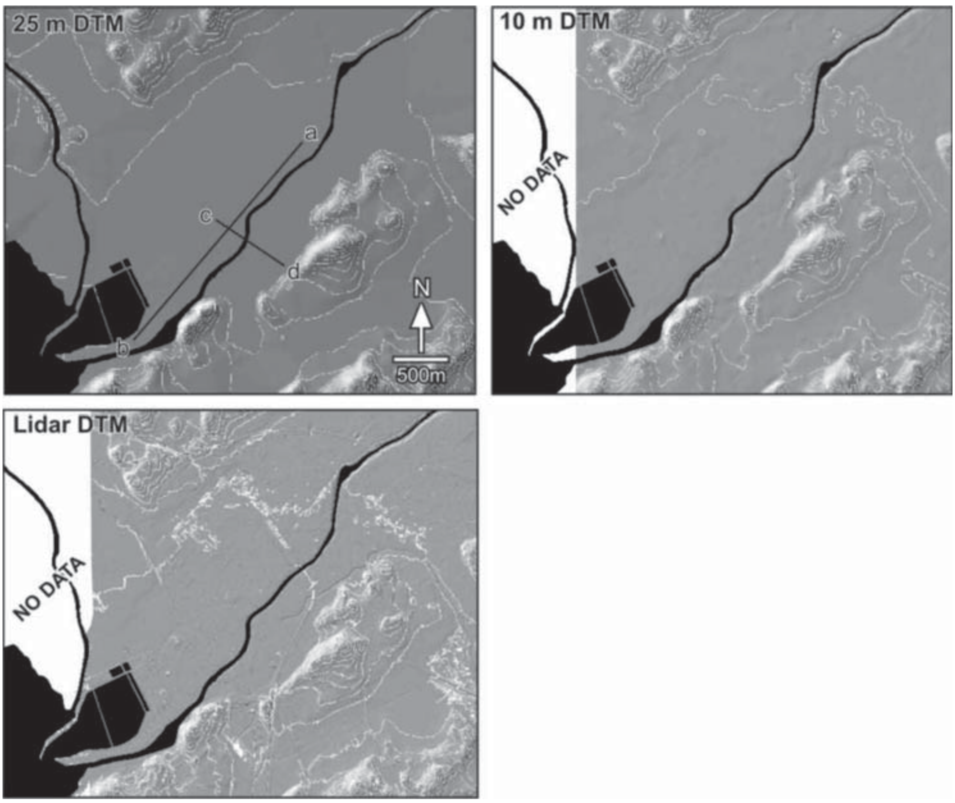

Figure 2. *Hillshade visualisation of the DTM's used in this study (25m DTM; 10 m DTM; Lidar DTM). The 5 m contours were visualised on the all three DTM's. Location of the elevation profile is shown on the 25 m DTM.*

***Table 1.** Accuracy assessment of the DTM's based on RTK-GPS points. (a) Accuracy including all 196 measured points (b) Accuracy without 17 points that were surveyed on riverbanks (all showed a difference of more than ± 40 cm between the LiDAR DTM and RTK-GPS points).*

a.

	Max.	**Min**	**Average**	**St. Dev.**
Lidar DTM	0.73	–0.60	0.06	0.19
10 m DTM	2.86	–2.08	0.23	0.81
25 m DTM	3.77	–7.61	–2.06	1.79

b.

	Max.	**Min**	**Average**	**St. Dev.**
Lidar DTM	0.39	– 0.35	0.05	0.12
10 m DTM	2.86	– 1.37	0.24	0.79
25 m DTM	3.77	– 6.89	– 1.91	1.75

4.2 Comparison of variations in elevation between DTM's

A comparison of elevation values between the LiDAR and 25 m digital terrain models indicated that the upstream reach of the 25 m DTM was markedly elevated, i.e. the 25 m DTM lay at an elevation of 5 m on both the whole upstream bank section and the city centre (Fig. 3A), which was between 1.0–2.8 m too high compared to the LiDAR DTM. Furthermore, the midstream section was also at a similar level and only decreased in the nearby Viurilanlahti Bay.

An elevation DTM profile analysis also indicated a flat 5 m section parallel to the river (Fig 4). The 25 m DTM was so generalised that it did not represent any embankment and the riverbank was also poorly modelled. In Fig. 4, the profile

***Figure 3A-B.** Difference images of the LiDAR DTM vs. 25 m DTM (A) and LiDAR DTM vs. 10 m DTM (B). The difference images were processed without bathymetric data. The black dots with elevation values (m) on both images represent elevation differences between LiDAR DTM and 25 m DTM (A) and LiDAR DTM and 10 m DTM (B). See table 2 for further statistics of the DTM comparisons.*

'a–b' shows that most of the western riverbank elevation was level at 5 m and the slope of the 25 m DTM was totally flat. In addition, the profile 'c–d' in Fig. 4 indicated that no features of the riverbanks were represented in the terrain model. In general, the whole model was flat and too elevated in the Salo region. The highest and lowest difference values between the LiDAR- and 25 m DTM's was 25.78 and 19.56 m, respectively (Table 2, Fig. 3A), while the standard deviation of the difference image was 1.99 m.

Elevations of the upstream bank section were better modelled in the 10 m DTM than in the 25 m DTM, ranging from 0.3–1.2 m too high, compared to the LiDAR DTM. However, the elevation was excessive in the 10 m DTM also (Table 2, Fig. 3). Some of the largest features were represented on the 10 m DTM (Fig 3). For example, elevation profile analysis showed that although the railway embankment was recognisable (Fig. 4, profile 'a–b'), it was modelled 60 cm too low compared to the LiDAR DTM. The slope trend of the 10 m DTM was similar compared to the LiDAR DTM, nevertheless, a number of erroneous elevations were recognised, i.e. ±1.5 m. Fig. 4. profile 'c–d' indicated that although the riverbanks were modelled in the 10 m DTM, they were sloped when they should be vertical in this section. The most positive and negative difference values of the 10 m DTM were 14.26 m and –9.97 m, respectively (Fig 3B). The standard deviation of the difference image elevations was 0.98 m (Table 2).

Table 2. *Statistics of the difference images. The 10 m DTM had better accuracy than the 25 m DTM compared to LiDAR DTM.*

	Lidar DTM vs. 25 m DTM (m)	**Lidar DTM vs. 10 m DTM (m)**
Higher	25.78	14.26
Lower	19.56	9.97
Average	–1.01	0.06
St. Dev.	1.99	0.98

4.3 Differences in flood inundation maps

A steady flow calculation for a discharge of 165 $m^3 s^{-1}$ was carried out using the geometry of three different DTM's in conjunction with HEC-RAS 4.0 hydraulic modelling software. Three sets of channel and floodplain cross-sections were extracted from these digital terrain models and used in water surface calculations. Subsequently, water surface elevations were interpolated to the whole reach and merged with the various DTM's to model flood inundation areas.

The inundation map of the 25 m DTM was highly erroneous, due to the lack of the inclined elevations towards Viurilanlahti Bay. In addition, the only bank elevations of the 25 m DTM were artificially created by the additional bathymetric data in the geometry to enable flow calculations in the channel. Therefore, in places, the modelled flood overflowed the riverbank, e.g., by the waste management plant (Fig. 5). These areas were mainly inundated by a 91 $m^3 s^{-1}$ discharge (HQ 1/35a) that occurred in early January 2005 (used in the calibration of the hydraulic model, cf. section 3.4). The pixel size of the 25m DTM also affects the visualisation of

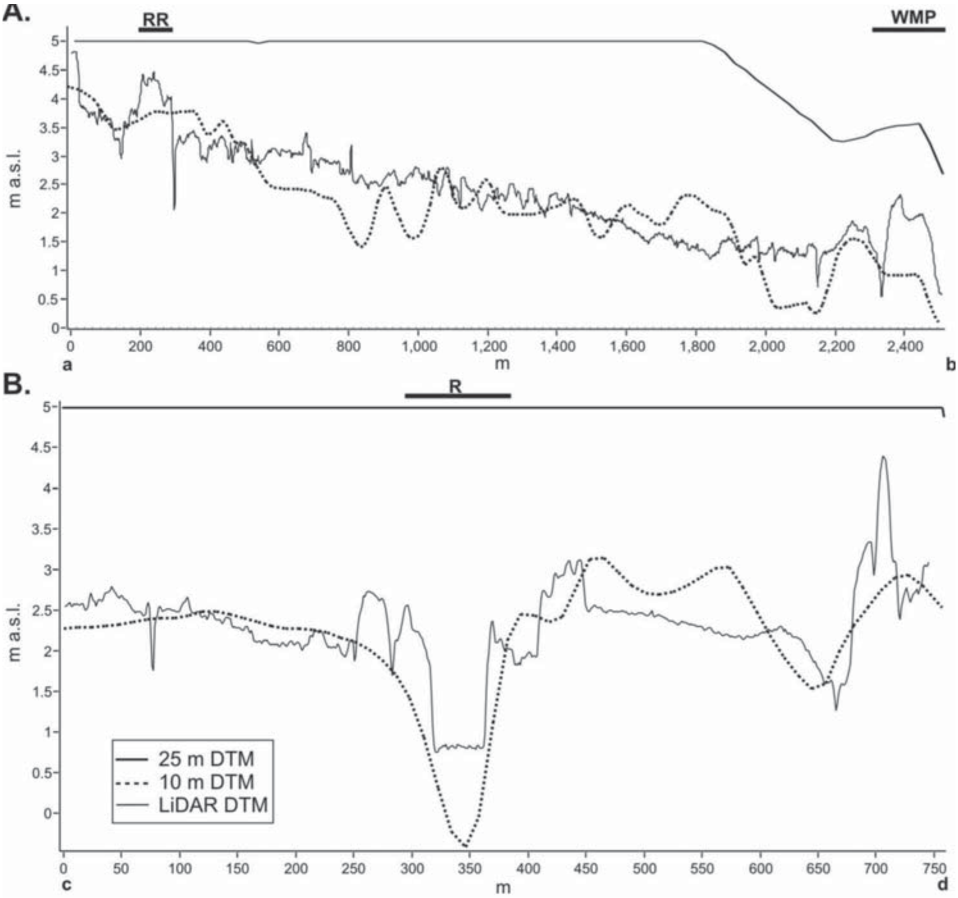

Figure 4. *Elevation profiles of the DTM's (locations of the profiles, see Fig. 2). A. The elevation profile 'a–b' indicates that no slope was modelled towards Viurilahti Bay in the 25 m DTM. The 10 m DTM showed this slope, but there was still a notable difference in elevation between the 10 m- and LiDAR DTM. The rail road embankment is highlighted with the letters "RR" and waste management plant with WMP. B. The elevation profile 'c–d' shows that the 25 m DTM is totally flat without any riverbank features. The 10 m DTM represented riverbanks at the right site, but they were inclined. Riverbanks are highlighted by the letter "R" and black thick line. Elevation profiles were prepared without bathymetric data.*

the flood map. Thus, the extent of the flood inundation boundaries was considered approximate at best. Flood depths were logically inaccurate, ranging from 0.01 to 1.32 m and were too low for the inundated area with a discharge of 165 $m^3 s^{-1}$.

The 10 m DTM allowed for a more detailed flood inundation mapping than the 25 m digital terrain model (Fig. 6), with the inundation mapping of a 1/35a flood event closely reflecting water surface levels of the actual event mentioned above. Furthermore, a 1/100a inundation map of the 10 m DTM was quite similar to its LiDAR DTM counterpart. A one-dimensional hydraulic modelling approach created floodwater ponds that had no connection to the flooded channel (Fig. 7 &

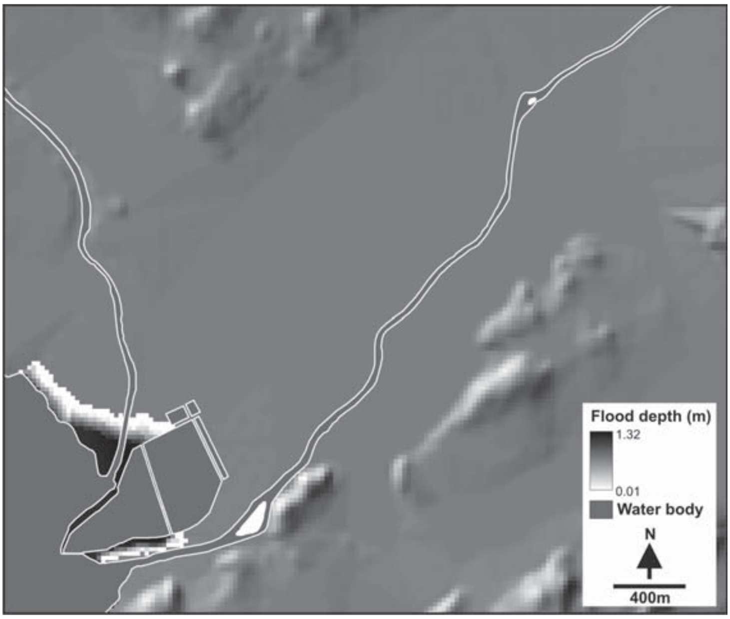

Figure 5. *A flood inundation map based on the 25 m DTM. The flat, high level areas in the mid- and upstream reaches prevented the correct merging of the modelled water surface elevation with the topography. The waste management plant is located nearby on the square-type water body (Note, islands in the river were not mapped).*

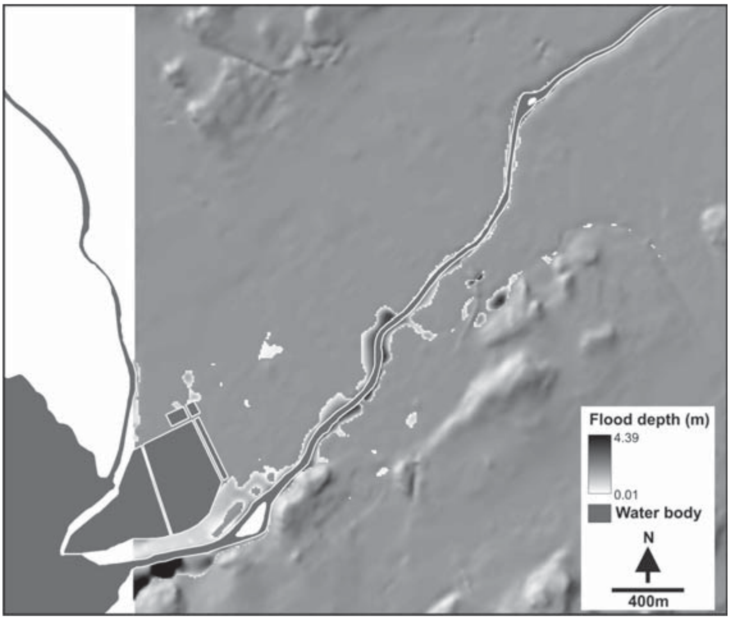

Figure 6. *A flood inundation map based on the 10 m DTM. The flat, high-level areas mid- and upstream did not allow for the correct merging of the modelled water surface elevation to the topography (Note, islands in the river were not mapped and "flood ponds" were not removed from the inundated area).*

8). These "flood ponds" were not cleared manually from these flood hazard maps in this study as it was considered appropriate to show a raw flood inundation map. A number of these ponds may occur in reality through the sewer network. Nowadays, a practical flood hazard mapping procedure includes the clearing of all such ponds (cf. Sane et al., 2006).

The best match to the flood inundation map of the 10 m DTM to the flood inundation map of the LiDAR DTM was found along the downstream reaches. Notable areas with excessive depths were also found in this digital terrain model, compared to the LiDAR DTM, ranging from 0.01 to 4.39 m for the entire inundation area, and was 1.05 m deeper than the inundation map of the LiDAR DTM counterpart (Fig. 7).

The flood inundation map created with LiDAR DTM geometry was the most accurate flood inundation map in this study (Fig. 7). The calibration of the hydraulic model with the 1/35a year flood also showed a good match. The differences of the flood boundary varied horizontally from 1 to 3 m, with *ca.* 10 cm differences in water surface elevation. These dissimilarities were most probably caused by the hydraulic modelling approach used and thus it was impossible to carry out a more accurate calibration (cf. Hydrologic Engineering Centre, 2001).

The flood map based on the LiDAR DTM gave a detailed picture of the possible inundation of a 1/100a flood. The topography was so accurate that the

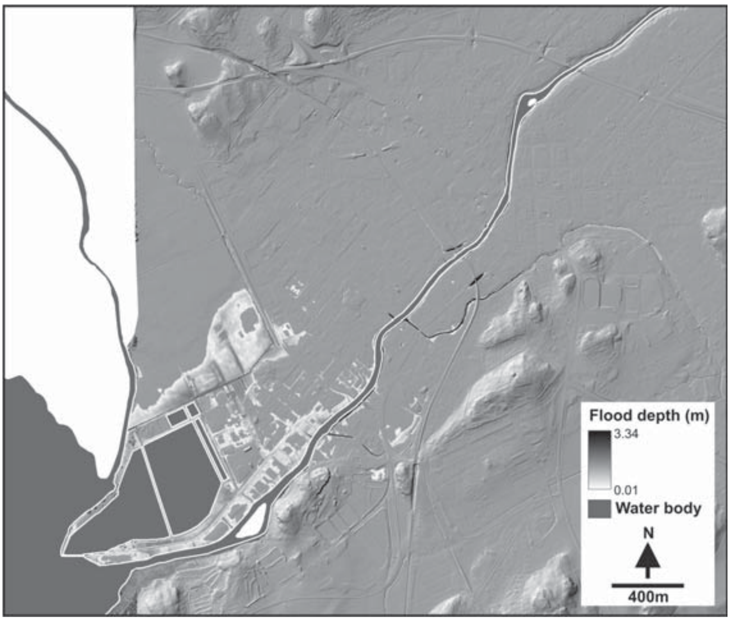

Figure 7. *A flood inundation map based on the LiDAR DTM (1m grid). The flat, high-level areas mid- and upstream prevented the correct merging of the modelled water surface elevation to the topography (Note, islands in the river were not mapped and "flood ponds" were not removed from the inundated area).*

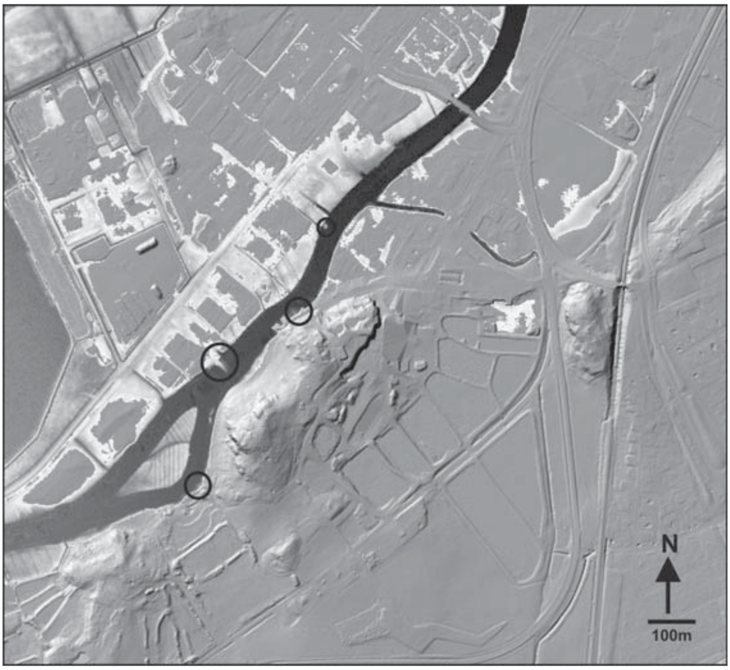

Figure 8. *A subset of the LiDAR DTM flood inundation map along the downstream section. The damming effects of the embankments and flood water on the dykes were easily recognised. Flood water ponds and their possible connection to the river could also be analysed. Some erroneous riverbanks are highlighted with black circles.*

inundation of a single ditch could be detected. Moreover, ditches that connected a flood area, e.g. from a flooded field north of the waste water management plant to the main channel, could be identified from the flood inundation map (Fig. 7 & 8). Even the topography of road embankments could also be perceived and thus, how they were affected by the flooding. Furthermore, inundated roads could be mapped and an accurate estimation of the flood depth on the roads given.

The inaccuracy of bank geometry in the LiDAR DTM affected the flood mapping slightly (cf. Table 1 and Fig. 8). Elevated square areas were detected on the river and some bank areas which showed incorrectly tilting slopes (highlighted with black circle in Fig. 8). The LiDAR data in the Salo area has been pre-processed with the water mask of the topographic database by NLS. Elevation of the water mask is based on the averaged values of the LiDAR points covered by the mask (Haikarainen 2007). If the real water surface elevation was larger during the laser scanning than the area covered by the water mask, the elevation of the riverbanks were defined by laser points reflected from the water surface. Furthermore, if the real water surface was smaller during the laser scanning than the area of the water mask, the averaged water surface elevation (based on LiDAR points under the water mask) was defined for water body and riverbanks. Thus, it is reasonable to propose that inaccuracies in riverbank inundation were due to the masking procedure in the LiDAR data pre-processing. However, because these errors were limited to the riverbanks, it can be stated that these data were generally well suited for flood inundation mapping.

5 Discussion

Flood hazard mapping is an essential part of flood mitigation (cf. European Union flood directive (Directive on 2007/60/EC…, 2007) and thus the accuracy of these maps is of vital importance, because flood damages are the most severe natural hazards in Europe. On the other hand, such areas are highly appreciated for housing due to their proximity to water. Therefore, it is important to develop better flood mapping tools for practical use and acquiring the high-precision topography for flood models is a crucial step in this development.

In this study, an accuracy assessment of the three digital terrain models and their applicability for one-dimensional flood inundation mapping clearly showed that LiDAR DTM topography was the most applicable (cf. Sanders, 2007 for Lidar DTM and Horritt and Bates, 2002 for 1D modelling approach). Although a 10×10 m DTM could be utilised in very coarse flood mapping to show where flooding might occur, it was not suitable for more exact estimations of flood boundaries. On the other hand, lower resolution DTM data such as a 10×10 m and 25×25 m DTM could be enhanced with break lines on river bank sections and floodplains (cf. Sane et al. 2006). This manipulation could improve input geometry of the hydraulic model and thereby modelling outcomes might be more accurate. However, surveying and processing of the additional data is time-consuming and spatial coverage of the additional data is quite often incomplete.

The LiDAR data enabled the creation of a flood map with detailed inundation routes, an accurate water depth analysis for the area of interest (roads, ditches, etc.), as well as an exact flood boundary. However, some inaccuracies were also found in LiDAR DTM: the most imprecise areas were riverbanks. This is a clear disadvantage for sophisticated flood modelling. The geometry of the riverbanks should be adjusted with additional data. Dynamic terrestrial laser scanning would be a potential approach to diminish these inaccuracies in selected areas. In addition, bathymetric data cannot be acquired with traditional laser scanning and therefore, the further development of new survey instruments is recommended.

Furthermore, more sophisticated flood modelling such as two-dimensional, depth-averaged hydrodynamic modelling would be appropriate to create more accurate flood maps in densely urbanized areas, where flow conditions are more complex than in rural areas (cf. Hunter et al. 2008). To validate which model-based flood ponds have the potential to occur in a real flood situation, the sewer network would also be useful information to add to the hydraulic model. Moreover, river channel dynamics, land uplift and the impacts of climate change should be also included in estimations of both future flow conditions and flood maps.

6 Conclusions and further research

This study compared three different digital terrain model products in flood hazard mapping. The following conclusions could be drawn:

1. There were extreme differences in flood mapping results, such that only two DTM products could be used in flood mapping: the topography of the 25×25 m DTM should not be used in flood mapping, while that of the 10×10 m DTM was only suitable for coarse flood mapping to show where, for example, a 1/100a flood might occur in the city of Salo. By comparison, the topography of the LiDAR DTM could be utilised in detailed flood hazard mapping.
2. The flood depth on important infrastructures such as roads could be analysed accurately using the flood map based on the high-accurate LiDAR DTM (ca. 2 m horizontal resolution or better). These accurate flood depths could be used as an input data for flood risk mapping. Furthermore, connective flow routes such as ditches between the main channel and the inundated areas could also be perceived in LiDAR DTM and 1D model in this case study. However, a multidimensional flow model would give better results in very densely urbanised areas with a sewer network (cf. Mignot et al., 2006).
3. Inaccuracies in the LiDAR DTM were found on the riverbanks. These incorrect elevation values of the banks were most probably caused by the masking procedure of the water bodies utilised (cf. Haikarainen 2007), which although justified over large scale LiDAR DTM production, may be problematic in highly detailed hydrological studies.
4. The LiDAR DTM could be processed as a DSM (digital surface model) and it was possible to recognise forested areas, buildings, etc. even from a low point density (i.e. 0.5 pt/m^2) of the laser point cloud. These specific geometric models enable sophisticated unsteady, multidimensional flow modelling on a very detailed scale.

While traditional laser scanning with a wavelength of red light gathers very accurate topography, it is not possible to undertake a bathymetric survey with such an instrument. Therefore, new devices should be tested to gather seamless, accurate 'fluvial-DTM' data. Potential approaches for this kind of DTM product which should be investigated include multi-wavelength laser scanning (red and green wavelengths) and parallel side-scan sonar surveys. Both normal and dynamic terrestrial laser scanning are also prospective approaches to improve riverbank topography, which gather long-term data sets for studying river dynamics and for validating two- and three-dimensional hydrodynamic models.

Acknowledgements. This study was supported by the Academy of Finland (post-doc research project, decision number: 115530 and Academy research fellow project, decision number: 124574) and by the EXTREFLOOD II research project funded by the Ministry of Agriculture and Forestry and the Ministry of the Environment. The National Land Survey of Finland is acknowledged for providing the DTM data for this study.

References

Ahokas, E., Kaartinen, H., Hyyppä, J. (2008). On the quality checking of the airborne laser scanning-based nation wide elevation model in Finland, submitted to ISPRS Congress, Beijing, 2008

Ahokas, E., Kaartinen, H., Matikainen, L., Hyyppä, J., Hyyppä, H. (2002). Accuracy of high-pulse-rate laser scanners for digital target models. In: Observing our environment from space. New solutions for a new millennium. In *Proceedings of the 21st EARSeL Symposium*, 14–16 May 2001, Paris, Balkema Publishers, pp. 175–178.

Alho, P., Sane, M., Lotsari, E., Lehtiö, L., Huokuna, M., Käyhkö, J. (2008). Tulvariskien kartoittaminen. (Guidebook for flood risk mapping). 99 pp. Ympäristöhallinnon ohjeita 2 Finnish Environment Institute, Helsinki.

Alho, P., Aaltonen, J., Käyhkö, J., Veijalainen, N., Selin, M., Harilainen, L., Tarvainen, V. (2007). Flood scenario studies in SW Finland. Proceedings in The 3rd International Conference on Climate and water, 3.–6.9.2007, Helsinki. Finnish Environment Institute, pp. 19–24.

Alsdorf, D.E., Melack, J.M., Dunne, T., Mertes, L.A.K., Hess, L.L., Smith, L.C. (2000). Interferometric radar measurements of water level changes on the Amazon flood plain. *Nature* 404, pp. 174–177.

Axelsson, P. (2000). DEM Generation from Laser Scanner Data Using Adaptive TIN Models. In IAPRS. Vol. 33. part B4/1, pp. 110–117.

Bates, P. D. (2004). Remote sensing and flood inundation modelling. *Hydrological Processes* 18, pp. 2593–2597.

Bates, P. D., Marks, K. J., Horritt, M. S. (2003). Optimal use of high-resolution topographic data in flood inundation models. *Hydrological Processes* 17, pp. 537–557.

Chow, V., 1959. *Open-channel hydraulics.* 699 pp. McGraw-Hill, New York.

Cobby, D.M., Mason, D.C. and Davenport, I.J. (2001). Image processing of airborne scanning laser altimetry data for improved river flood modelling. *ISPRS Journal of Photogrammetry & Remote Sensing* 67, pp.121−138.

Dartmouth Flood Observatory. (2005). www.dartmouth.edu/~floods/Archives/2005sum.html [ref. 24.1.2008]

Directive on 2007/60/EC on the assessment and management of flood risks. (2007). An EU policy on flood risk management. http://eur-lex.europa.eu/LexUriServ/LexUriServ.do?uri=OJ:L:2007:288:027:0034:EN:PDF [ref. 24.1.2008]

EC. (2005). Towards a European Action programme on flood risk management. http://europa.eu.int/comm/environment/water/flood_risk. [ref. 20.1.2008]

Fisher, P., Tate, T. (2006). Causes and consequences of error in digital elevation models. *Progress in physical Geography* 30, pp. 467–489.

Floodsite (2005). Language of risk – Project definitions. Floodsite consortium report, T32-04-01, 56 pp, http://www.floodsite.net/html/partner_area/project_docs/FLOODsite_Language_of_Risk_v4_0_P1(1).pdf. [ref. 3.10.2008].

Haikarainen, J. (2007). *Uuden korkeusmallin tarkkuus ja parametrit* (Accuracy and parameters of the new DTM). Suurten alueiden laserkeilauksen testityö workshop presentation, Pasila, Helsinki 22.11.2007. http://www.maanmittauslaitos.fi/Tietoa_maasta/Ilmakuvaus/Korkeusmalliseminaari_22.11.2007/. [ref. 4.1.2008.]

Horritt, M. S. Bates, P. D. (2002). Evaluation of 1D and 2D numerical models for predicting river flood inundation. *Journal of Hydrology* 268, pp. 87–99.

Hudson, P.F., Colditz, R.R. (2003). Flood delineation in a large and complex alluvial valley, lower Pánuco basin, Mexico. *Journal of Hydrology* 280, pp. 229–245.

Hunter, N., Bates, P., Neelz, S., Pender, G., Villanueva, I., Wright, N., Liang, D., Falconer, R., Lin, B., Waller, S. Crossley, A., Mason, D. (2008). Benchmarking of 2D hydraulic models for urban flooding. *Water Management* 161, pp. 13–30.

Hydrologic Engineering Centre (2002). *HEC-RAS River analysis system. Hydraulic Reference Manual ver. 3.1* . Army Corps of Engineering, California.

Hyyppä, H., Yu, X., Hyyppä, J., Kaartinen, H., Honkavaara, E., Rönnholm, P. (2005). Factors affecting the quality of DTM generation in forested areas. In *Proceedings of ISPRS Workshop Laser scanning 2005*, September 12–14, 2005, Enschede, Netherlands, (Netherlands: GITC bv), XXXVI (Part 3/W19), pp. 85–90.

Kenward, T. Lettenmaier, D. Wood, E. Fielding, E. (2000). Effects of Digital Elevation Model Accuracy on Hydrologic Predictions. *Remote Sensing of Environment* 74, pp. 432–444.

Ludwig, R., Schneider, P. (2006). Validation of digital elevation models from SRTM X-SAR for applications in hydrologic modeling. *ISPRS Journal of Photogrammetry and Remote Sensing* 60, pp. 339–358.

Mignot, E., Paquier, A., Haider, S. (2006). Modelling floods in a dense urban area using 2D shallow water equations. *Journal of Hydrology* 327, pp. 186–199.

NLS (2007). *Korkeusmalli 25:n tarkkuusanalyysi*. (25 m DEM accuracy assessment). http://www.maanmittauslaitos.fi/tarkkuusanalyysi.htm [ref. 20.1. 2008]

Oksanen, J., and Sarjakoski, T., (2006). Uncovering the statistical and spatial characteristics of fine toposcale DEM error. *International Journal of Geographical Information Science*, 20(4), pp. 345–369.

Ollila, M., Virta, H. and Hyvärinen V. (2000). *Suurtulvaselvitys. Arvio mahdollisen suurtulvan aiheuttamista vahingoista Suomessa.* (Report on extreme floods; assessment of the damage caused by a potential extreme flood in Finland). *Suomen Ympäristö* 441, 138 pp. Finnish Environment Institute.

Reutebuch, S., McGaughey, R., Andersen, H. and Carson, W. (2003). Accuracy of a high-resolution lidar terrain model under a conifer forest canopy. *Can. J. Remote Sensing,* 29, pp. 527–535.

Sanders, B. (2007). Evaluation of on-line DEMs for flood inundation modeling. *Advances in Water Resources* 30, pp. 1831–1843.

Sane, M., Alho, P., Huokuna, M., Käyhkö, J., Selin, M. (2005). *Opas yleispiirteisen tulvavaarakartoituksen laatimiseen* (Guidelines for flood hazard mapping on a coarse scale). 73 pp. Environment Guide 127, Finnish Environment Institute, Helsinki.

Schumann, G., Matgen, P., Cutler, M.E.J., Black, Hoffmann, A.L., Pfister, L. (2008), Comparison of remotely sensed water stages from LiDAR, topographic contours and SRTM, *ISPRS Journal of Photogrammetry and Remote Sensing* 63, pp. 283–296.

Sithole, G., and Vosselman, G. (2004). Experimental comparison of filter algorithms for bare-Earth extraction from airborne laser scanning point clouds. *ISPRS Journal of Photogrammetry and Remote Sensing* 59, pp. 85–101.

Takeda, H. (2004). Ground surface estimation in dense forest. *The International Archives of Photogrammetry, Remote Sensing and Spatial Information Sciences*, Vol. 35, part B3, pp. 1016–1023.

Veijalainen, N. (2005). *Extreflood: Ilmastonmuutoksen vaikutus kerran 100 ja kerran 250 vuodessa toistuviin tulviin*. (Extreflood: The effect of climate change on floods recurring once every 100 and once every 250 years) EXTREFLOOD I report, Finnish Environment Institute, Helsinki.

Veijalainen, N., Vehviläinen, B. (2007). *Ilmastonmuutoksen vaikutukset mitoitustulviin* (The effects of climate change on design floods). *Vesitalous*, pp. 9–12.